Inter*net* **Electronic** Journal of 𝔐𝔬𝔩𝔢𝔠𝔲𝔩𝔞𝔯 𝔇𝔢𝔰𝔦𝔤𝔫

June 2008, Volume 7, Number 6, Pages 131–141

Editor: Ovidiu Ivanciuc

Docking and QSAR Studies for Inhibitors of Thymidylate Synthase

Kotni Meena Kumari,[1] Sivan Sree Kanth,[1] and Manga Vijjulatha [1]

[1] Department of Chemistry, Nizam College, Osmania University, Basheer Bagh, 500 001 Hyderabad, India

Citation of the article:
K. M. Kumari, S. S. Kanth, and M. Vijjulatha, Docking and QSAR Studies for Inhibitors of Thymidylate Synthase, *Internet Electron. J. Mol. Des.* **2008**, *7*, 131–141, http://www.biochempress.com.

Docking and QSAR Studies for Inhibitors of Thymidylate Synthase

Kotni Meena Kumari,[1] Sivan Sree Kanth,[1] and Manga Vijjulatha [1,*]

[1] Department of Chemistry, Nizam College, Osmania University, Basheer Bagh, 500 001 Hyderabad, India

Abstract

A series of novel antifolate inhibitors having naphthalene core, substituted quinazoline, indole, pyrrolo–pyrimidine, pyrido–pyrimidine, and pteridine were designed using computational technique. These molecules were compared with the known classical and non–classical antifolate inhibitors of the thymidylate synthase by performing docking studies and by computing their ADME properties. The designed molecules showed good binding affinity towards the protein compared to the several thymidylate synthase inhibitors. The biological activities for these inhibitors were predicted withy a model equation generated by regression analysis between biological activity (pK_i) of known inhibitors and there E–model which is a specific combination of Glide score, Coulombic and van der Waals interactions. The MLR QSAR analysis was carried out on 20 analogues used as training set, and 8 analogues used as test set. This study gave a reasonably good predictive model with R^2 = 0.957 and R^2_{LOO} = 0.871 (leave–one–out method). The cross validation on the test set gave R^2_{cv} = 0.587 and RMS = 0.493.

Keywords. Thymidylate synthase; ADME; docking; activity; QSAR; quantitative structure–activity relationships; E–model.

Abbreviations and notations	
ADME, absorption, distribution, metabolism, and elimination	OPLS–AA, optimized potentials for liquid simulations
DM, dipole moment	Polrz, polarizability
MR, molar Refractivity	QSAR, quantitative structure–activity relationships
MMFF94s, Merck molecular force field 94 static	SASA, solvent accessible surface area

1 INTRODUCTION

Thymidylate synthase (TS) [1] is especially attractive as a target for therapeutic interventions since cellular DNA synthesis cannot be maintained in the absence of functioning thymidylate synthase because the transfer of the one–carbon moiety from 5,10–methylene tetrahydrofolate to deoxy uridylate occurs concomitantly with the oxidation of the cofactor tetrahydrofolate to the dihydrofolate level. Thymidylate synthase catalyzes the reductive methylation of deoxyuridylate to deoxythymidylate that is required for the pyrimidine nucleotide biosynthesis later produced in the

---

* Correspondence author; E–mail: drmvl2002@yahoo.com.

DNA synthesis [2]. Thus inhibition of TS is an attractive target for the development of antitumor agents.

Several classical antifolates inhibitors, notably ZD1694 [3], LY231514 [4], PDDF [5], 10–propargyl–5,8–dideazafolic acid (Quin–1) [6,7] contain a benzoyl L–glutamic acid side chain which acts as the substrate for folypoly–γ–glutamate synthetase (FPGS). FPGS catalyzes the formation of poly–γ–glutamate [4,5,8] leading to high intracellular concentrations of these antitumor agents and at the same time increases the TS inhibitory activity. In the case of the classical inhibitors, a decrease in the FPGS activity can cause resistance and/or inefficient uptake. Examples of nonclassical analogue are TMQ [9,10] originally developed as an anticancer agent [11,12,13], AG337 [14] which is the first nonclassical TS inhibitor to reach clinical trials, Quin–2 to Quin–20 [6] that are not dependent on FPGS for their potency and could passively diffuse into cells. These classical and non–classical inhibitors of thymidylate synthase were clinically active but had toxic effects [15]. Therefore it is important to design novel potent TS inhibiting drugs, which will be more soluble, having ability to passively diffuse into the cell and non–toxic in nature. In the present work both the classical and the non–classical antifolate inhibitors of thymidylate synthase (TS) were taken into consideration, and we performed docking and QSAR studies on them. The novel classical folate analogues were designed by using the napthalene core and by substitution on the existing quinazoline, indole, pyrrolo–pyrimidine, pyrido–pyrimidine and pteridine cores, while maintaining required ADME properties.

2 MATERIALS AND METHODS

The computational work was run on a 3.2 GHz Intel Pentium–IV system. The software Glide 4.0 [16] was used for protein preparation, protein minimization, grid generation and ligand docking. QikProp 2.5 [17] was used to calculate the ADME properties of the ligands, the existing ligands (quinazolines) with their K_i values were obtained from Jones *et al.* [6]. Thymidylate synthase crystal structure was downloaded from protein data bank (PDB 1HVY) [18]. The protein structure was prepared by glide application's protein preparation job. Protein minimization was carried out using a conjugate gradient method applying a convergence gradient of 0.01 kcal/mol. The OPLS–AA force field was used for this purpose and then the active site of the protein was defined and a grid was prepared for the protein structure with receptor van der Waals scaling for the non polar atoms as 0.9. The ligands were built and prepared by using Ligprep 2.0 application, which produces the low energy conformer of the ligand using the MMFF94s force field. The ADME properties and molecular descriptors were calculated by using QikProp 2.5. The low energy conformations of the ligands were selected, these were then docked into the protein using the standard precision docking mode [19].

quin 1

quin 2, 3, 4, 7, 9, 10, 11, 13 - 20, 23, 25, 27, 28

2. R = 3 - CF$_3$,4 - SO$_2$NH - CH$_2$COOH

3. R = 4 - SO$_2$ - NH$_2$

4. R = 3 - CF$_3$, 4 - SO$_2$NH$_2$

7. R = 4 - CO - C$_6$H$_5$

9. R = 3 - CF$_3$, 4 - NO$_2$

10. R = 3 − C≡CH

11. R = 3 - Cl, 4 - CN

13. R = 3 - Br

14. R = 4 - Cl

15. R = 3 - CH$_2$OH

16. R = 4 - CN

17. R = 3 - CH$_3$

18. R = 3 - I

19. R = 3 - CF$_3$

20. R = H

23. R = 4 - SO$_2$ - C$_6$H$_5$

25. R = 4 - SO$_2$ - CF$_3$

27. R = 3 - C$_2$H$_5$

28. R = 3 - CF$_3$ 4 - CN

quin 5

quin 6

quin 8

quin 21

quin 12

quin 22, 24, 26

22. X = O

24. X = NH

26. X = N - CH$_3$

Figure 1. Structures of the quinazoline molecules.

3 RESULTS AND DISCUSSION

Quinazoline inhibitors were taken from literature [6] and have a wide range of inhibition constants (Figure 1). Their ADME properties were calculated using QikProp 2.5. The required pharmacokinetics properties [20,21] for a viable drug are: molecular weight should be in the range of 150 to 650 amu, partition coefficient (log Po/w) should be greater than −1 and less than +6.5, solubility (log units) should be greater than −7 and number of metabolic reactions should be less than 10.

A QSAR model was generated using the Strike 2.5 application, for the known quinazoline molecules (descriptors values given in Tables 1 and 2, calculated with QikProp), using the MLR

method which gave a good predictive model with $R^2 = 0.957$ and $R^2_{LOO} = 0.871$ with leave–one–out method. The cross validation on the test set gave $R^2 = 0.587$. Scatter plot of predicted activity vs experimental activity is shown in Figure 2.

$$pK_i = -0.139 + 0.043(\pm0.015)\ MR + 0.011(\pm0.026)\ DM + 0.015(\pm0.054)\ SASA$$
$$- 0.228(\pm0.091)\ Polrz - 0.465\ (\pm0.166)\ Log\ Po/w - 0.518\ (\pm0.173)\ Log\ S$$
$$n = 20 \quad R = 0.98 \quad R^2 = 0.957 \quad F = 48.0 \quad SEE = 0.186 \quad PRESS = 0.424\ p < 0.00001$$
$$R^2_{LOO} = 0.871 \quad test\ set\ n = 8 \quad R^2_{cv} = 0.587 \quad PRESS = 1.949 \quad RMS = 0.493$$

(1)

Table 1. Calculated descriptors of quinazoline molecules from the training set

Mol	MR	DM	SASA	Polrz	Log Po/w	Log S	E–model	Glide Score	$pK_{i\ exp}$	$pK_{i\ pre}$
Quin–1	124.27	4.06	812.39	47.74	2.48	−5.56	−140.9	−11.63	8.15	8.04
Quin–2	121.49	9.94	771.52	45.84	2.61	−5.63	−114.3	−10.70	7.73	7.79
Quin–3	104.67	11.44	671.44	38.51	1.57	−4.32	−80.3	−9.35	7.07	7.08
Quin–4	109.43	13.02	703.70	41.19	2.38	−5.25	−80.2	−9.46	7.15	7.27
Quin–5	123.25	8.96	730.41	46.29	3.51	−5.55	−78.6	−9.09	6.89	6.68
Quin–6	132.62	9.75	769.77	48.20	3.83	−6.13	−78.2	−9.00	7.07	7.39
Quin–7	123.57	5.39	752.82	46.78	4.64	−6.55	−76.9	−8.91	6.79	6.87
Quin–8	126.89	6.46	760.58	47.40	3.95	−5.58	−69.1	−8.66	6.96	6.81
Quin–9	103.42	13.13	685.58	40.14	4.12	−6.34	−63.8	−8.36	6.82	6.75
Quin–10	102.04	4.23	648.27	37.79	4.13	−5.46	−61.6	−7.42	6.17	6.12
Quin–11	104.13	10.45	628.88	36.57	3.30	−5.98	−60.4	−8.13	7.10	6.92
Quin–12	98.67	9.89	648.69	38.49	3.62	−5.54	−60.2	−8.24	6.31	6.15
Quin–13	100.56	4.50	616.68	36.27	4.16	−5.47	−60.2	−7.25	6.07	5.92
Quin–14	97.6	5.923	625.15	36.43	4.15	−5.61	−60.0	−8.12	6.11	5.98
Quin–15	98.47	4.47	610.46	35.19	2.85	−4.10	−58.7	−7.81	5.92	5.89
Quin–16	99.53	9.68	638.97	36.75	3.05	−5.87	−57.4	−7.83	6.77	6.88
Quin–17	97.43	3.44	602.67	35.56	3.85	−4.88	−57.0	−7.90	5.47	5.57
Quin–18	105.66	5.86	639.19	37.43	4.36	−5.94	−54.9	−7.73	6.36	6.38
Quin–19	97.76	7.43	653.05	38.465	4.63	−6.32	−52.7	−7.91	5.96	6.09
Quin–20	93.00	3.88	601.13	35.12	3.70	−4.85	−50.9	−7.21	5.24	5.52

Scatter plot of Experimental pKi vs Predicted pKi
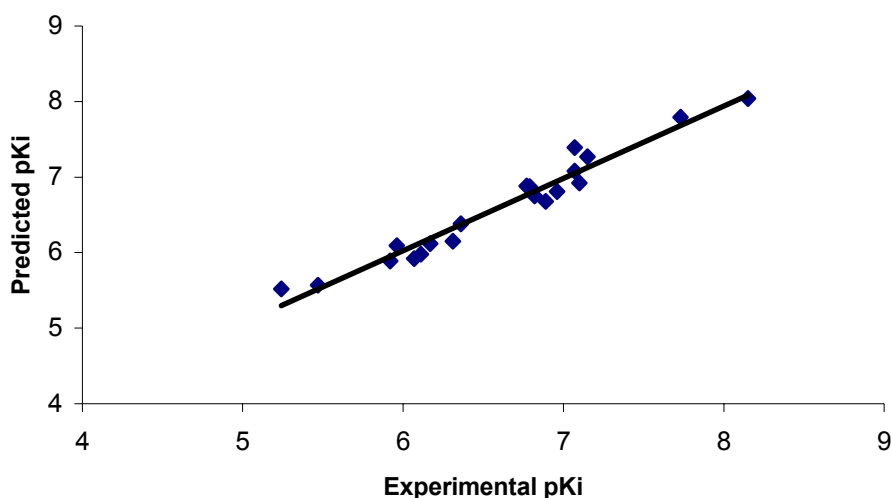
Figure 2. Scatter plot of experimental pK_i vs predicted pK_i.

Table 2. Calculated descriptors of quinazoline molecules from the test set

Mol	MR	DM	SASA	Polrz	Log Po/w	Log S	E–model	Glide Score	$pK_{i\,exp}$	$pK_{i\,pre}$
Quin–21	113.22	10.77	716.03	44.58	2.94	−5.54	−77.9	−8.84	5.66	6.71
Quin–22	123.99	7.06	722.58	44.76	2.49	−4.53	−77.7	−9.12	7.04	6.87
Quin–23	127.86	7.74	770.02	48.21	3.83	−6.13	−77.7	−9.00	7.68	7.16
Quin–24	125.66	6.42	761.42	46.46	2.03	−3.98	−75.7	−9.06	7.15	7.06
Quin–25	107.51	10.58	704.11	41.74	3.09	−5.65	−68.7	−8.90	7.55	6.92
Quin–26	130.98	6.12	775.35	48.28	2.34	−3.96	−63.9	−7.92	6.72	6.91
Quin–27	102.04	3.92	632.94	37.56	4.31	−5.26	−60.0	−8.15	5.42	5.75
Quin–28	104.28	11.52	649.03	38.43	3.79	−6.53	−58.1	−8.05	6.85	6.87

These molecules were docked into the protein (PDB: 1HVY) having the active site amino acids (Arg50, Lys77, Phe80, Asn112, Leu221, Asn226, Met309). The top molecules of this series *i.e.* Quin–1, Quin–2, Quin–3, Quin–4 having inhibition constant 0.0071, 0.019, 0.084, 0.070 μM showed the docking score of −11.63, −10.70, −9.35, −9.46, and E–model being −140.9, −114.3, −80.3, −80.2 kcal/mol respectively (Table 1). The cores of these 4 molecules showed hydrogen bond interactions with Lys77 and the side chain interacting with Asn226 of the active site and also interacting with the other amino acid like Ile307 which is not there in the active site, where as it did not show any interactions with the other active site amino acids.

For the rest of the molecules in the series the core only interacted with Lys77 and very few molecules showed the side chain interactions with Asn226 and these molecules had E–model value very less compared to Quin–1, Quin–2, Quin–3, and Quin–4. The correlation of E–model vs biological activity (pK_i) of the known inhibitors gave correlation coefficient $R = 0.80261$ and standard error of estimate SEE = 0.4393, the following equation was derived with the scatter plot of biological activity vs E–model shown in Figure 3:

$$pK_i = -0.02612\,(E\text{–model}) + 4.79862 \qquad (2)$$
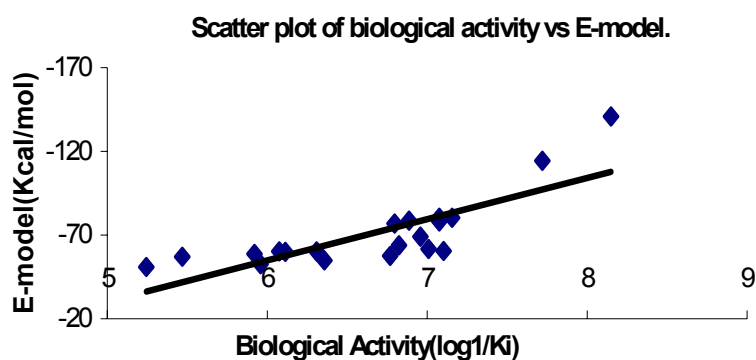
Figure 3. Scatter plots of biological activity vs E–model.

The new molecules were computationally designed using 6 different cores having substituents at N–10 position for naphthalene, quinazoline, pyrido pyrimidine and pteridine cores, and substitution

at N–9 position for indole and pyrrolo pyrimidine cores (Figure 4). These molecules were first screened for their drug like properties *i.e.* ADME using QikProp 2.5 and were docked into the protein (PDB: 1HVY) active site which showed the E–model greater than the known molecules. The molecules (M–1 to M–67) showed the highest E–model value compared to the known molecules.
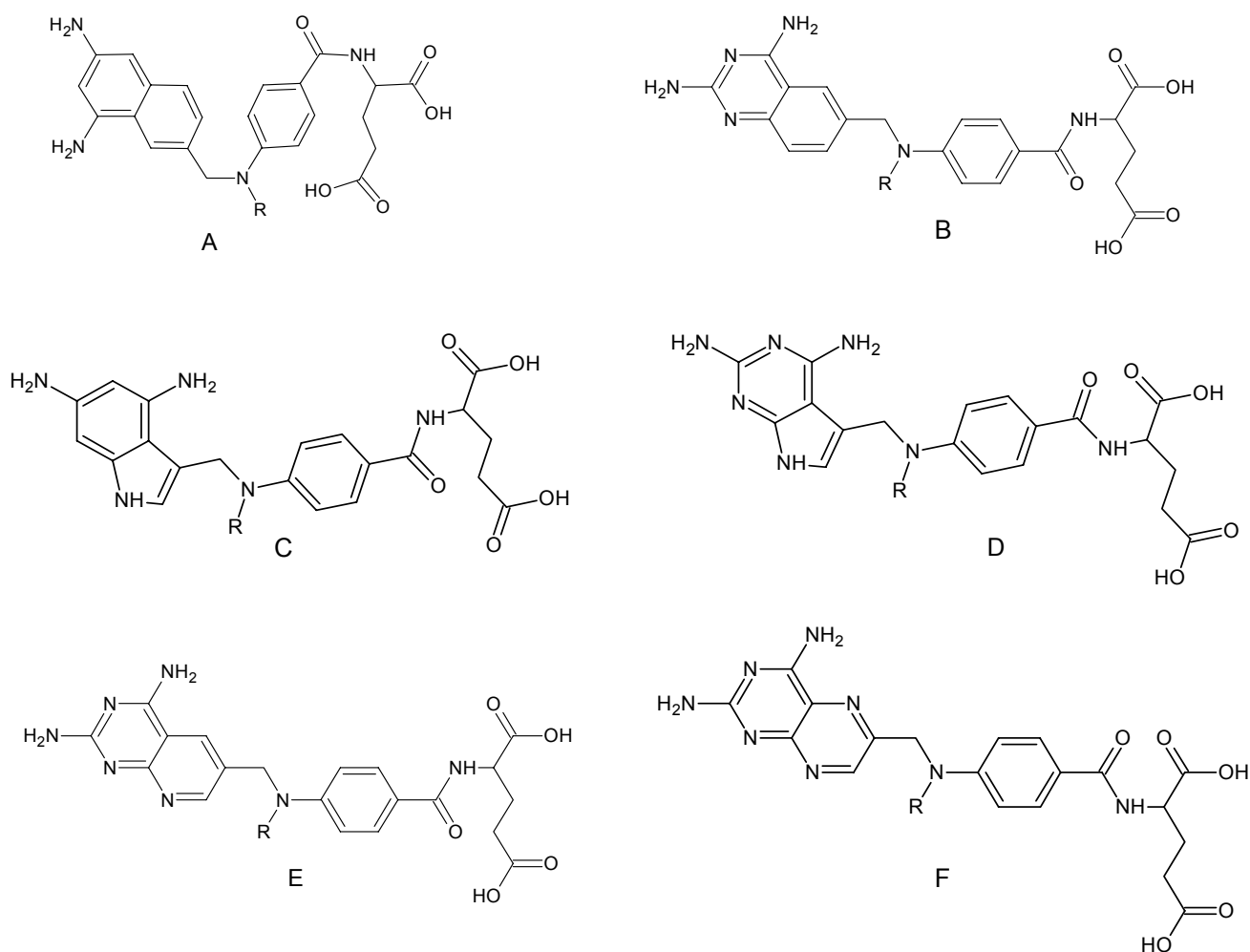
A = Napthalene core, B = Quinazoline core, C = Indole core, D = Pyrrolo pyrimidine core, E = Pyrido pyrimidine core,   F = Pteridine core.

Figure 4. Structures of newly designed molecules.

The cores of designed molecules (Figure 5) showed interactions with Asn112 and Leu 221 and the substituent on N–10 and N –9 position interacted with Asn226 and Arg50 of the active site, α–carboxylic acid of glutamic acid interacted with Phe80 and γ–carboxylic acid interacted with Lys77.

They also showed interactions with the other amino acids like Arg215, Asp218, Tyr135, Tyr258 which are not there in the active site. (Hydrogen bonding shown in yellow color, active site amino acids shown in pink color with ball and stick representation, ligand shown in tube form and the protein is shown in ribbon model).

Substitutions at position N-10 for A, B, E, F (R)

Substitutions at position N-9 for C,D (R)
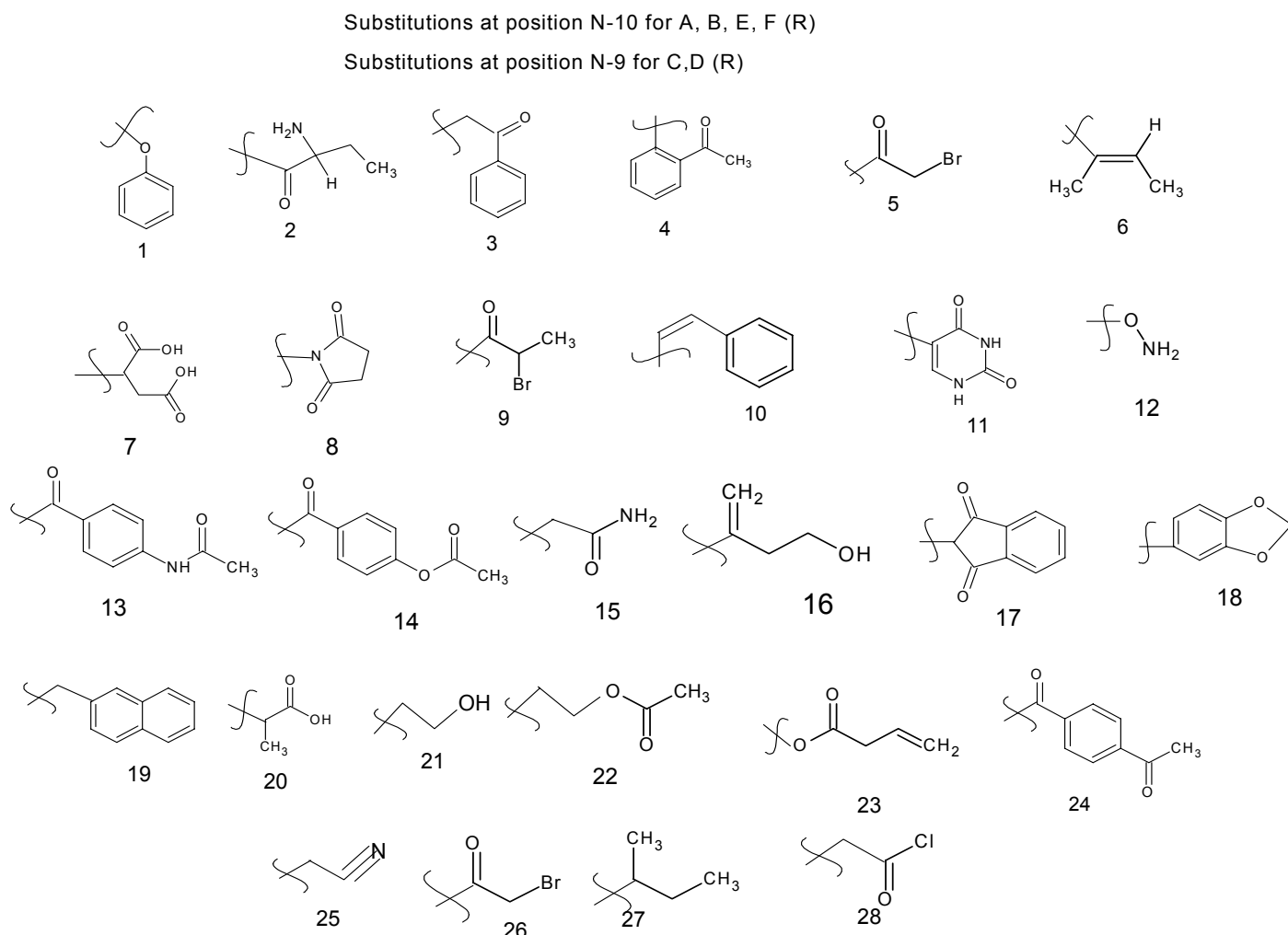
Figure 4. (Continued).

The cores of designed molecules (Figure 5) shows interactions with Asn112 and Leu 221 and the substituent on N–10 and N –9 position interacted with Asn226 and Arg50 of the active site, α–carboxylic acid of glutamic acid interacted with Phe80 and γ–carboxylic acid interacted with Lys77. They also showed interactions with the other amino acids like Arg215, Asp218, Tyr135, Tyr258 which are not there in the active site. (Hydrogen bonding shown in yellow color, active site amino acids shown in pink color with ball and stick representation, ligand shown in tube form and the protein is shown in ribbon model).

Table 3. Calculated descriptors, E–model, Glide score, and predicted activity for the new molecules

Mol	Core	R	MR	DM	SASA	Polrz	LogPo/w	LogS	E–model	Glide Score	$pK_{i\,pre}$
M–1	F	24	161.6	11.82	935.42	57.69	2.178	–6.38	–179.9	–12.50	9.83
M–2	A	7	143.59	1.93	827.48	48.74	0.41	–4.18	–170.7	–11.50	9.08
M–3	D	24	152.22	3.06	890.37	53.24	0.46	–5.21	–170.6	–11.73	9.87
M–4	C	7	138.03	7.58	766.30	44.74	–0.13	–3.22	–167.5	–9.66	8.67
M–5	F	14	155.28	7.09	897.04	55.58	0.14	–4.80	–167.4	–10.23	9.55
M–6	F	13	158.21	4.14	946.34	56.78	–0.10	–5.44	–166.7	–11.27	10.54
M–7	C	11	139.41	14.12	806.14	47.98	0.24	–4.41	–164.8	–10.90	9.10
M–8	B	13	162.03	6.29	953.15	57.99	1.01	–6.03	–164.3	–11.22	10.34
M–9	C	13	160.28	3.60	936.88	57.12	1.41	–6.02	–160.5	–11.73	10.00
M–10	C	4	150.83	7.48	829.81	51.34	2.38	–5.21	–159.0	–11.18	8.51
M–11	E	17	152.93	11.94	846.64	52.78	0.31	–4.60	–157.4	–10.91	9.22
M–12	B	14	159.1	8.02	930.53	57.21	1.21	–5.79	–157.3	–10.80	9.86
M–13	D	19	159.55	4.98	877.97	54.94	2.74	–5.90	–152.3	–10.07	8.94
M–14	B	17	154.84	8.42	835.02	52.92	0.88	–4.66	–151.9	–9.76	8.82
M–15	C	21	127.21	8.22	772.28	43.13	0.78	–3.98	–151.6	–9.28	8.64
M–16	F	23	134.37	3.62	817.91	47.35	0.17	–3.98	–151.4	–10.04	8.89
M–17	A	4	156.4	10.97	868.43	54.39	3.05	–5.98	–151.3	–11.28	8.74
M–18	D	11	135.59	6.33	790.34	46.22	–0.81	–3.89	–151.2	–10.03	9.23
M–19	B	15	130.99	7.36	798.87	45.02	–0.97	–2.90	–151.0	–10.09	9.01
M–20	E	3	150.48	4.31	893.88	53.30	1.473	–5.45	–150.7	–9.32	9.50
M–21	D	10	148.05	4.80	866.46	52.03	2.23	–5.72	–150.5	–11.61	9.08
M–22	E	19	161.76	6.35	904.87	56.81	2.89	–6.28	–150.5	–10.23	9.14
M–23	F	1	140.59	10.20	823.38	49.25	1.05	–4.67	–150.4	–9.94	8.82
M–24	B	9	139.77	9.01	819.31	48.23	1.21	–5.09	–149.7	–10.42	9.09
M–25	B	20	133.58	6.84	778.58	45.32	0.55	–4.00	–149.7	–9.52	8.61
M–26	D	16	132.22	3.73	772.75	43.74	0.27	–3.51	–149.1	–10.80	8.67
M–27	C	23	136.44	6.02	807.89	47.10	1.44	–4.49	–149.1	–10.15	8.59
M–28	F	28	128.48	9.52	795.35	44.45	–0.29	–4.21	–148.5	–10.62	9.37
M–29	E	22	136.55	2.99	846.54	47.78	0.48	–4.74	–148.4	–9.96	9.55
M–30	E	9	137.87	6.15	802.94	46.71	0.49	–4.69	–148.4	–9.49	9.22
M–31	B	10	153.62	6.65	895.81	54.66	2.94	–6.38	–147.8	–10.59	9.18
M–32	C	22	136.71	7.49	809.45	46.85	1.62	–4.62	–147.5	–10.31	8.68
M–33	B	1	144.41	7.45	837.99	50.68	2.14	–5.34	–147.4	–10.04	8.68
M–34	F	4	148.76	7.42	827.72	50.69	0.87	–4.51	–147.3	–10.45	8.87
M–35	E	11	139.25	11.32	843.14	48.82	–0.79	–4.57	–147.2	–11.06	9.97
M–36	B	16	137.79	3.56	814.89	46.09	0.98	–4.26	–146.9	–10.03	9.05
M–37	F	12	111.62	6.92	768.97	41.57	–0.97	–3.58	–146.8	–10.36	9.22
M–38	A	5	139.0	6.81	811.15	47.92	2.07	–5.41	–146.6	–10.37	8.75
M–39	D	8	132.86	6.42	820.79	46.84	–0.13	–4.57	–146.4	–11.35	9.46
M–40	C	16	136.04	7.63	774.59	44.58	1.37	–3.85	–146.2	–10.10	8.38
M–41	D	23	132.62	3.18	795.61	45.47	0.44	–3.99	–146.0	–10.63	9.58
M–42	B	7	139.77	3.59	797.75	46.70	–0.34	–3.48	–145.4	–9.07	8.95
M–43	E	26	134.31	11.62	812.08	45.99	0.37	–4.90	–145.3	–10.31	9.58
M–44	E	20	131.67	2.72	779.13	44.99	–0.06	–3.83	–144.2	–9.48	8.76
M–45	F	10	149.8	8.63	886.85	53.28	1.77	–5.75	–143.7	–9.68	9.44
M–46	B	19	165.12	5.84	924.70	58.35	3.61	–6.85	–143.7	–9.02	9.18
M–47	F	22	134.64	2.96	854.04	48.17	0.25	–4.61	–143.6	–9.89	9.53
M–48	B	12	123.44	9.89	769.24	42.45	0.06	–3.89	–143.5	–9.95	8.89
M–49	C	14	157.35	7.74	941.59	57.79	1.78	–6.22	–143.3	–9.97	9.77
M–50	A	2	144.03	5.21	839.79	49.13	–0.82	–4.29	–143.3	–9.55	9.86
M–51	F	3	148.57	4.95	886.15	53.12	1.08	–5.09	–143.1	–10.38	9.35
M–52	B	18	148.71	5.96	852.46	52.07	2.56	–5.84	–143.1	–10.09	8.81
M–53	D	12	117.87	3.28	719.18	39.22	–0.45	–3.05	–143.0	–9.82	8.39
M–54	D	1	138.84	4.70	796.54	47.75	1.49	–4.54	–142.8	–9.75	8.36
M–55	B	11	141.16	12.56	833.14	49.46	–0.08	–4.62	–142.7	–8.94	9.47
M–56	B	3	152.39	8.18	912.56	54.73	2.04	–5.99	–142.5	–9.53	9.59

Table 3. (Continued)

Mol	Core	R	MR	DM	SASA	Polrz	LogPo/w	LogS	E–model	Glide Score	p$K_{i\,pre}$
M–57	B	8	138.43	4.24	841.61	49.18	0.53	–4.98	–142.4	–10.32	9.35
M–58	C	18	146.97	8.34	809.36	49.88	2.38	–5.16	–141.8	–10.50	8.36
M–59	D	26	129.62	6.68	775.74	43.59	0.29	–4.47	–141.8	–9.75	9.15
M–60	F	19	161.3	4.44	899.37	56.07	2.21	–5.94	–141.8	–9.70	9.33
M–61	A	6	140.4	13.45	817.35	49.28	2.92	–5.69	–141.5	–10.18	8.41
M–62	E	12	121.53	6.97	768.49	41.79	–0.52	–3.73	–141.5	–9.61	9.11
M–63	E	27	135.77	11.97	820.21	46.90	1.32	–4.95	–141.2	–9.86	9.14
M–64	A	8	142.24	8.23	850.14	50.89	1.63	–5.46	–141.1	–10.51	9.03
M–65	A	1	148.22	12.94	845.54	52.15	3.17	–5.86	–141.1	–9.94	8.48
M–66	D	25	121.77	8.04	731.41	40.83	–0.06	–4.43	–141.1	–9.75	8.95
M–67	A	3	156.2	5.60	853.49	53.24	2.75	–5.45	–140.9	–10.37	8.59
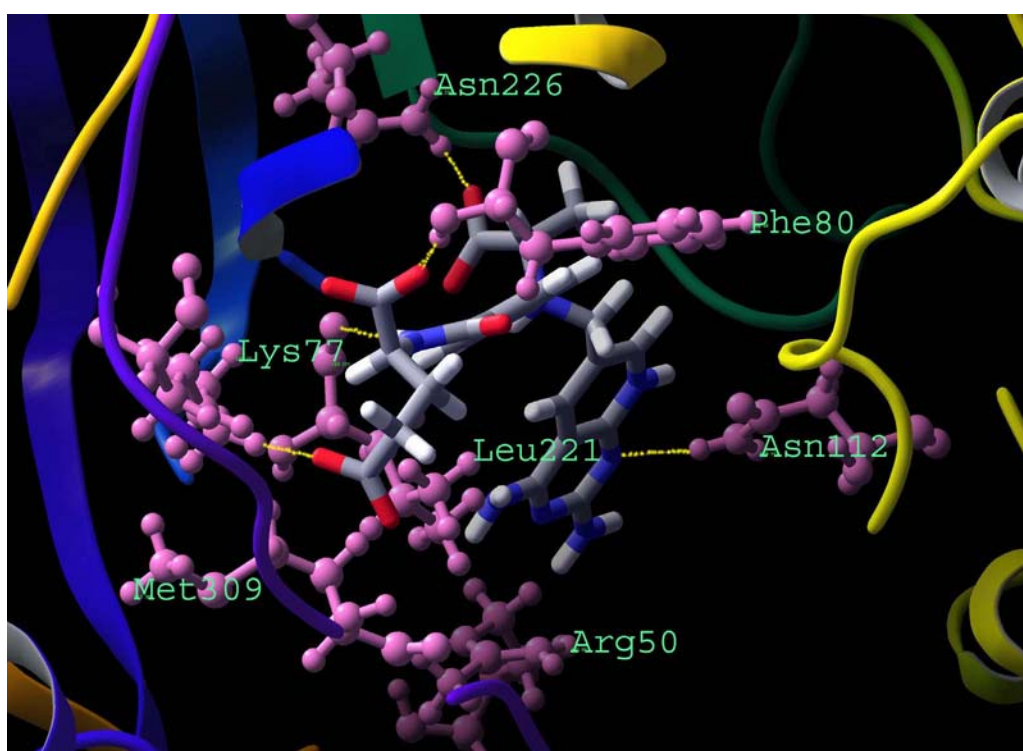
Figure 5. The designed molecules showing hydrogen bonding interaction with the active site amino acids of thymidylate synthase.

The designed molecules activity has been predicted using the model equation (Eq. 1) generated from the existing molecules. This showed that the designed molecules are having better predicted activity than that of the known molecules (see Table 3 for descriptor values, E–model and predicted activity).

4 CONCLUSIONS

In the current docking studies of the known quinazoline inhibitors and the newly designed molecules it is established that the newly designed molecules showed good binding affinity, which is evident from E–model value and glide score. Amongst the 67 molecules M–1 showed a highest

E–Model and glide score (−179.9 Kcal/mol, −12.5 respectively). QSAR study gave a good statistical model with R^2 of 0.957, $R^2_{cv/LOO}$ of 0.871 and R^2_{cv} of 0.587 on test set. Predicted activities of new molecules using the QSAR model were better compared to the known inhibitors. Hence these newly designed molecules can be considered as the hit molecules. Compounds like M– 1, 3, 6, 8, 9,12, 43 that have good E–model and predicted activity can be considered as hit molecules. There synthetic studies are in progress.

Acknowledgment

5 REFERENCES

[1] S. S. Cohen and H. D. Barner, *Proc. Natl. Acad. Sci.*, *U. S. A.* **1954**, *40*, 885–893.
[2] J. S. Colin, Enzyme Chemistry: Impact and Applications, In: Enzymes as targets for drug design, Eds.:B. Hesp and A. K. Wilard, 1984, pp–121–127, Chapman and Hall, NY.
[3] A. L Jackman, G. A. Taylor, W. Gibson, R. Kimbell, M. Brown, A. H. Calvert, I. R. Judson, L. R. Hughes, A Quinazoline Antifolate Thymidylate Synthase Inhibitor That is a Potent Inhibitor of L1210 Tumor Cell Growth in vitro and in vivo: A New Agent for Clinical Study, *Cancer Res*. **1991**, *51*, 5579.
[4] E. C. Taylor, D. Kuhnt, C. Shih, S. M. Rinzel, G. B. Grindey, J. Barredo, M. Jannatipour, R. A. Moran, A Dideazatetrahydrofolate Analogue Lacking a Chiral Center at C–6, N–[4–[2–(2–amino–3,4–dihydro–4–oxo–7H–pyrrolo[2,3–d]pyrimidin–5–yl)ethyl]benzoyl]–L–glutamic acid, is an Inhibitor of Thymidylate Synthase, *J.Med.Chem*. **1992**, *35*, 4450.
[5] T. R. Jones, A. H. Calvert, A. L. Jackman, S. J. Brown, M. Jones, K. R Harrap, A Potent Antitumor Quinazoline Inhibitor of Thymidylate Synthase: Synthesis, Biological Properties and Therapeutic Results in Mice, *Eur. J. Cancer* **1981**, *17*, 11.
[6] T. R. Jones, M. D. Varney, S. E. Webber, K. K. Lewis, G. P. Marzoni, C. L. Palmer, V. Kathardekar, K. M. Welsh, S. Webber, D. A. Matthews, K. Appelt, W. W. Smith, C. A. Janson, J. E. Villafranca, R. J. Bacquet, E. F. Howland, Carol L. J. Booth, Steven M. Herrmann, R. W. ward, J. White, E. W. Moomaw, C. A. Bartlett, and C. A. Morse, Structure–Based Design of Lipophilic Quinazoline Inhibitors of Thymidylate Synthase, *J. Med. Chem*. **1996**, *39*, 904–917.
[7] T. R. Jones, T. J. Thornton, A. Flinn, A. L. Jackman, D. R. Newell, A. H Calvert, Quinazoline Antifolates Inhibiting Thymidylate Synthase: 2–Desamino Derivatives with Enhanced Solubility and Potency. *J. Med. Chem*. **1989**, *32*, 847–852.
[8] A. Gangjee, H. D. Jain, and R. L. Kisliuk, Novel 2–amino–4–oxo–5arylthio–substituted–pyrrolo[2,3–d]pyrimidines as nonclassical antifolate inhibitors of thymidylate synthase, *Bioorg. Med. Chem. Lett*. **2005**, *15*, 2225–2230.
[9] E. F. Elslager and J. Davoll, In: Lectures in Heterocyclic Chemistry. 2, Castle, R. N.; Townsend, L. B., Eds.; Hetero corp. Orem: UT, 1974, pp S97–S133.
[10] E. F. Elslager, J. L. Johnson, and L. M. Werbel, Folate Antagonists. 20. Synthesis and Antitumor and Antimalarial Properties of Trimetrexate and related 6–[(phenylamino)ethyl]–2,4–quinazolinediamines, *J. Med. Chem*. **1983**, *26*, 1753–1760.
[11] J. R. Bertino, W. L. Sawacki, B. A. Moroson, A. R. Cashmore, and E. F. Elslager, *Biochem. Pharmacol*. **1979**, *28*, 1983–1987.
[12] E. C. Weir, A. R. Cashmore, R. N. Dreyer, M. L. Graham, N. Hsiao, B. A. Moroson, W. L. Sawacki, and J. R. Bertino, Pharmacology and Toxicity of a Potent "Nonclassical" 2,4–Diaminoquinazoline Folate Antagonist, Trimetrexate, in Normal Dogs, *Cancer Res*. **1982**, *42*, 1696–1702.
[13] J. T. Lin, A. R. Cashmore, M. Baker, R. N. Dreyer, M. Ernstoff, J. C. Marsh, J. R. Bertino, L. R. Whitfield, R. Delap, and A. Grillo–Lopez, Phase I Studies with Trimetrexate: Clinical Pharmacology, Analytical Methodology and Pharmacokinetics, *Cancer Res*. **1987**, *47*, 609–616.
[14] S. E Webber, T. M. Bleckman, J. Attard, J. G. Deal, V. Katherdekar, K. M. Welsh, S. Webber, C. A. Janson, D.

A. Matthews, W. W. Smith, S. T. Freer, S. R. Jordan, R. J. Bacquet, E. F. Howland, C. J. L. Booth, R. W. Ward, S. M. Hermann, J. White, C. A. Morce, J. A. Hilliard, and C. A. Bartlett, *J. Med.Chem.***1993**, *36*, 733.

[15] D. I Jodrell, D. R. Newell, S. E. Morgan, S. Clinton, J. P. M. Bensted, L. R. Hughes, and A. H. Calvert, The renal effects of N^{10}–propargyl–5,8–dideazafolic acid (CB3717) and a non–nephrotoxic analogue ICI D1694 in mice. *Br. J. Cancer* **1991**, *64*, 833–838.

[16] Schrödinger, LLC, New York, NY, **2005**. Glide, version 4.0.

[17] QikProp, version 2.5, Schrödinger, LLC, New York, NY, **2005**.

[18] J. Phan, S. Koli, W. Minor, R. B. Dunlap, S. M. Berger, and L. Lebioda. Human thymidylate synthase is in the closed conformation when complexed dUMP and raltitrexed, an antifolate drug, *Biochemistry* **2001**, *40*, 1897–1902.

[19] R. A. Friesner, J. L. Banks, R. B. Murphy, T. A. Halgren, J. J. Klicic, D. T. Mainz, M. P. Repasky, E. H. Knoll, M. Shelley, J. K. Perry, D. E. Shaw, P. Francis, and P. S. Shenkin, Glide: A New Approach for Rapid, Accurate Docking and Scoring. 1. Method and Assessment of Docking Accuracy, *J. Med. Chem.* **2004**, *47*, 1739–174.

[20] C. A. Lipinski, F. Lombardo, B. W. Dominy, and P. J. Feeney, Experimental and computational approaches to estimate solubility and permeability in drug discovery and development settings, *Adv. Drug. Deliver. Rev.* **1997**, *23*, 3–25.

[21] C. A. Lipinski, F. Lombardo, B. W. Dominy, and P. J. Feeney, Experimental and computational approaches to estimate solubility and permeability in drug discovery and development settings, *Adv. Drug. Deliver. Rev.* **2001**, *46*, 3–26.

Biographies

M. **Vijjulatha** M.Sc., Ph.D, is Senior Assistant Professor of chemistry at Osmania University. She obtained her Ph.D. degree in Inorganic chemistry from the University of Hyderabad, India under the supervision of Professor K. C. Kumar Swamy.

Kotni Meena Kumari and **Sivan Sreekanth** are research scholars pursing their Ph. D in Osmania University.